JCTC Journal of Chemical Theory and Computation

Describing Both Dispersion Interactions and Electronic Structure Using Density Functional Theory: The Case of Metal−Phthalocyanine Dimers

Noa Marom,[†] Alexandre Tkatchenko,[‡] Matthias Scheffler,[‡] and Leeor Kronik*,[†]

Department of Materials and Interfaces, Weizmann Institute of Science, Rehovoth 76100, Israel, and Fritz-Haber-Institut der Max-Planck-Gesellschaft, Faradayweg 4−6, 14195 Berlin, Germany

Received August 7, 2009

Abstract: Noncovalent interactions, of which London dispersion is an important special case, are essential to many fields of chemistry. However, treatment of London dispersion is inherently outside the reach of (semi)local approximations to the exchange-correlation functional as well as of conventional hybrid density functionals based on semilocal correlation. Here, we offer an approach that provides a treatment of both dispersive interactions and the electronic structure within a computationally tractable scheme. The approach is based on adding the leading interatomic London dispersion term via pairwise ion−ion interactions to a suitably chosen nonempirical hybrid functional, with the dispersion coefficients and van der Waals radii determined from first-principles using the recently proposed "TS-vdW" scheme (Tkatchenko, A.; Scheffler, M. *Phys. Rev. Lett.* **2009**, *102*, 073005). This is demonstrated via the important special case of weakly bound metal−phthalocyanine dimers. The performance of our approach is additionally compared to that of the semiempirical M06 functional. We find that both the PBE-hybrid+vdW functional and the M06 functional predict the electronic structure and the equilibrium geometry well, but with significant differences in the binding energy and in their asymptotic behavior.

1. Introduction

Noncovalent interactions, of which London dispersion is an important special case, are essential to many fields of chemistry. Such interactions possess a significant component of electrostatic attraction between permanent or instantaneous dipoles and higher order multipoles and dominate in regions where there is little overlap of charge densities, i.e., at medium-range to long-range, as compared to the short-range chemical bond. In principle, exact density functional theory (DFT) should include accurate treatment of the long-range correlation, which is essential for describing noncovalent interactions.[1] However, van der Waals (vdW) interactions (a term that we use here interchangeably with London dispersion) are inherently outside the reach of (semi)local approximations to the exchange-correlation (xc) functional as well as of conventional hybrid functionals, based on semilocal correlation.[1,2]

Many strategies toward inclusion of van der Waals interactions in DFT calculations, at various levels of approximation, have been proposed. Many of those can be divided into three broad categories: (1) nonempirical methods, typically relying on the adiabatic connection theorem,[3] where the long-range correlation is either computed explicitly[4−11] or integrated with traditional xc functionals;[12,13] (2) semiempirically parametrized xc functionals, calibrated for data sets that include noncovalently interacting systems;[14−18] (3) pairwise addition of C_6/R^6 corrections to the internuclear energy expression, damped in the short-range while providing the desired long-range asymptotic behavior.[19−28] Such C_6/R^6 corrections are usually semiempirical but can be derived from first-principles considerations.[28]

Understandably, most of the literature on DFT computations of dispersively bound systems has focused on obtaining

* Corresponding author phone: +972-8-934-4993; e-mail: leeor.kronik@weizmann.ac.il.

[†] Weizmann Institute of Science.

[‡] Fritz-Haber-Institut der Max-Planck-Gesellschaft.

10.1021/ct900410j
Published on Web 12/03/2009

correct geometries and binding energies. There are very important classes of systems, however, for which it is crucial to obtain a correct prediction of the electronic structure as well. An important example, on which we elaborate here, is that of small-molecule-based organic semiconductors. In such materials, intermolecular interaction in the molecular crystal is typically dispersive (or at least has a significant dispersion component), and geometry predicted using standard functionals can be highly inaccurate, as discussed, e.g., in ref 29. At the same time, an accurate description of the electronic structure is essential to understanding the relations between the chemical nature of the constituent molecules and their function in organic electronic devices.

A key question, then, is whether one can systematically obtain a sufficiently accurate theoretical treatment of both noncovalent interactions and the electronic structure, within a computationally tractable scheme that is preferably widely applicable and involves as little empiricism as possible. This is challenging because the electronic structure can be very sensitive to the type of functional used. A recurring reason for inadequate treatment of the electronic structure is the presence of self-interaction errors (SIE),[30,31] i.e., the spurious Coulomb interaction of an electron with itself in the Hartree term of the Kohn−Sham equation, which is not fully canceled out by approximate expressions for the exchange-correlation term. Local and semilocal functionals, e.g., the local-density approximation (LDA) and various flavors of the generalized gradient approximation (GGA), respectively, often exhibit significant SIE that results in a poor description of the electronic structure of organic molecules and crystals.[32,33] Hybrid xc functionals were found to mitigate the effect of the SIE significantly via the inclusion of a fraction of Fock exchange.[31−33] Therefore, a desirable scheme would combine a successful description of van der Waals interactions with a hybrid functional based description of the electronic structure.[34] This should be possible because the electronic structure is mostly sensitive to exchange and short-range correlation, whereas dispersive interactions mainly affect the total energies and geometries.

In principle, such a successful combination may be achieved within each of the three above-discussed strategies for treating van der Waals interactions. The most practical and successful representative of the first strategy (a nonempirical method relying on the adiabatic connection theorem) is the "vdW-DFT" functional of Dion et al.[13] (see ref 35 for some recent applications). It is based on a GGA (specifically revPBE[36]) exchange functional, combined with LDA for the local part of the correlation, on top of which the nonlocal correlation component is added. Although this nonlocal correlation can be combined with other functionals, results for, e.g., the binding energy may depend significantly on the underlying "parent" functional.[37] Therefore, we will not be discussing this approach here. Currently the most popular representative of the second strategy (semiempirical methods based on hybrid functionals) is the M06 family of functionals,[17] a family of meta-GGA functionals (i.e., functionals whose "semi-local" component includes kinetic energy spin-densities, in addition to the spin-densities and their gradients[31]) with varying fractions of exact exchange. This approach provides some flexibility in the choice of an appropriate functional, an issue elaborated below. However, the correct long-range R^{-6} behavior is still absent from such functionals even if medium-range noncovalent binding is well-achieved. The third strategy, addition of pairwise C_6/R^6 terms to the internuclear energy term, allows for the highest degree of flexibility in choosing independently the appropriate description of the electronic structure, on top of which a suitable dispersion correction is performed.

Obviously using C_6/R^6 corrections is not free from limitations either. First, the approach assumes that noncovalent interactions have little direct effect on the electron density and affect the system mainly by influencing the equilibrium geometry. Second, screening by the conduction electrons has to be addressed for metallic systems. Third, the short-range damping function may be problematic for the accurate description of short bond lengths. Fourth, Dobson et al.[38] have shown that summation over pairwise interactions may result in incorrect asymptotic behavior in certain special cases, e.g., low-dimensional (semi)metallic systems.

Here, we examine the degree to which a quantitative treatment of both the electronic structure and the dispersion interactions is achieved in practice. We show that this is indeed possible using the recently presented "TS-vdW" correction scheme,[28] in which the leading-order C_6 coefficients and vdW radii are determined in a first principles manner from the DFT ground-state electron density. These corrections are combined with the GGA of Perdew, Burke, and Ernzerhof (PBE)[39] with the one-parameter nonempirical PBE-hybrid (also known as PBEh or PBE0),[40] or with the three-parameter semi-empirical hybrid functional B3LYP.[41] We compare our results to those obtained from the M06 functional,[17] as well as to those obtained from the standard PBE and PBE-hybrid functionals and to pertinent experiments.

We have chosen two members of the metal−phthalocyanine (MPc) family as case studies for the above comparison, NiPc and MgPc. MPc's are highly stable organic semiconductors with a broad range of applications in, e.g., light emitting diodes, solar cells, gas sensors, thin film transistors, and even single molecule devices.[42] Specifically, their electronic structure has been shown to be highly sensitive to self-interaction errors.[32] Furthermore, it is known that $\pi-\pi$ and $\pi-$d interactions, which possess a dispersive component and are attributed to nonlocal electron correlations that occur in systems with spatially close-lying π orbitals,[43] play an important role in the stacking of molecules in MPc crystals. In transition metal Pc's, such as NiPc, $\pi-$d interactions affect the intermolecular distance in the stack.[44] In crystalline MgPc, $\pi-\pi$ interactions not only affect the intermolecular distance but also lead to a structural change in the molecular subunit as the Mg atom deviates from the molecular plane and shifts toward the azamethine N of the adjacent molecule (see also Figure 1), so that the basic unit of the MgPc crystal is, in fact, a dimer.[45,46] Thus, both NiPc and MgPc provide stringent test cases for a treatment of both geometrical and electronic structure.

Here, we calculate the binding energy curves, geometry, and electronic structure of NiPc and MgPc dimers. We find

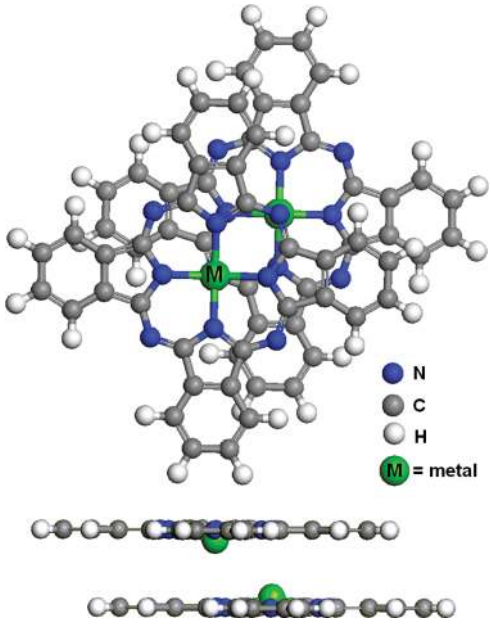

Figure 1. Schematic top-view and side-view of the MPc dimer. The metal atom of one molecule lies above the azamethine nitrogen of the other molecule. In the MgPc dimer, the Mg atom is shifted from the molecular plane, as shown in the side-view.

that PBE+vdW, PBE-hybrid+vdW, and M06 all yield similar geometries, but the electronic structure is well described only with the PBE-hybrid+vdW, the B3LYP+vdW,[47] and the M06 approaches. Moreover, we find significant differences in the binding energy between PBE-hybrid+vdW and M06. We attribute these differences to the long-range behavior of these two methods and show that they can be reduced by applying the TS-vdW C_6/R^6 correction to M06.

2. Methodology

a. TS-vdW Correction Scheme. In the TS-vdW[28] C_6/R^6 correction scheme used here, the pairwise vdW interaction, E_{disp}, added to the internuclear energy term, is given by

$$E_{\mathrm{disp}} = -\sum_{j>i} f_{\mathrm{damp}}(R_{ij}, R_{ij}^0) C_{6ij} R_{ij}^{-6} \qquad (1)$$

where C_{6ij} is the dispersion coefficient for the ij pair of atoms, R_{ij} is the interatomic distance, R_{ij}^0 is the sum of equilibrium vdW radii for the pair, and f_{damp} is a damping function discussed below. The novel feature of the TS-vdW scheme is that the parameters C_{6ij} and R_{ij}^0 are determined from first principles. The method yields significantly lower errors for the S22 database of molecular binding energies than empirical C_6/R^6 methods and has been recently shown to outperform the latter for water clusters.[48]

Briefly, the TS-vdW scheme is based on accurate *ab initio* computed reference values for free atom static dipole polarizabilities and C_6 coefficients,[49] a combination rule for deriving heteronuclear C_6 coefficients from homonuclear static dipole polarizabilities, and Hirshfeld partitioning[50–52] of the DFT electron density to calculate the relative polarizability of an atom inside a molecule. In this way, different atomic hybridization states are inherently taken into account for different molecular geometries. Complete details are given in ref 28.

The damping function in eq 1 is needed to avoid the divergence of the R^{-6} term at short distances and reduce the effect of the correction on covalent bonds. A Fermi-type function was used here, in the form

$$f_{\mathrm{damp}}(R_{ij}, R_{ij}^0) = \left[1 + \exp\left(-d\left(\frac{R_{ij}}{s_{\mathrm{R}} R_{ij}^0} - 1\right)\right)\right]^{-1} \qquad (2)$$

where d determines the "steepness" of the damping function and s_{R} reflects the range of interaction covered by the chosen DFT exchange-correlation functional.[25] By fitting to the S22 database of Jurečka et al.,[53] which contains binding energies of 22 different weakly bound systems close to CCSD(T) basis set limit, the value of d was set to 20 and s_{R} was set to 0.94 for PBE and 0.96 for the PBE-hybrid.[28,54] A similar procedure for B3LYP yielded an s_{R} of 0.84, indicating that a smaller range of dispersion interaction is covered, likely due to a somewhat more repulsive exchange component than that of PBE or the PBE-hybrid. Finally, as discussed by Karton et al.,[55] the M06 functional yields attraction at intermediate range but still does not possess the correct long-range behavior. Therefore, the same fitting procedure was performed for M06 as well, yielding the s_{R} value of 1.16.

b. Computational Details. The routines for evaluation of energies and forces using the TS-vdW method have been implemented in the FHI-aims code[56] for consistent geometry optimizations. FHI-aims is an all-electron electronic structure code developed at the Fritz Haber Institute. It uses efficient numerical atomic-centered orbitals (NAO) as a basis set and allows one to achieve highly converged results with optimum efficiency in computer resources. In this work, the tier2 NAO basis set, which yields results that are similar in accuracy to those of the aug-cc-pVQZ Gaussian basis set for the S22 database, has been employed for geometry relaxation.

Additional calculations of single molecule geometry and dimer geometry of MgPc and NiPc were performed using the Gaussian[57] code with the PBE, PBE-hybrid, B3LYP, and M06 functionals. Calculations of the electronic structure of a single NiPc molecule were performed using the revPBE functional, the functionals M06L and M062X of the M06 family, and BLYP[58]-based functionals with similar fractions of exact exchange. The Def2-TZVP Weigend−Ahlrichs basis set[59] was used for all calculations, except for the MgPc M06 calculations, for which a larger all-electron cc-pVTZ basis[60] was used. Throughout this work, the single molecule geometry was optimized independently for each functional and basis set.

Binding energy curves were constructed using the PBE, PBE-hybrid, B3LYP, and M06 functionals, with and without C_6/R^6 corrections. The counterpoise (CP) method[61,62] was used to correct for basis set superposition errors (BSSE). In order to obtain dimer binding energy curves as a function of a single parameter, the intermolecular distance was varied under the assumption that the metal atom of one molecule lies directly above the azamethine nitrogen of the other molecule,[44–46] and that the metal atom is in the molecular plane. The latter assumption is consistent with experimental

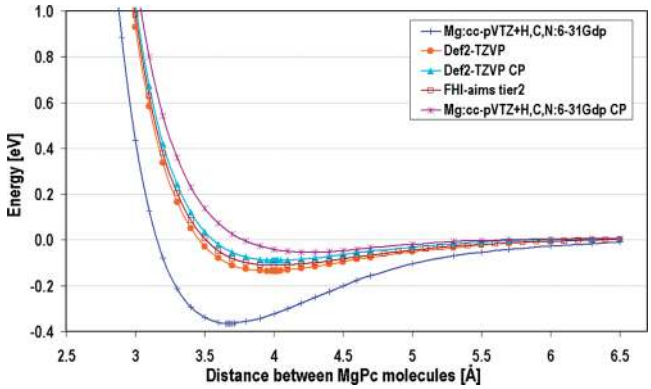

Figure 2. Binding energy curves for the MgPc dimer, obtained with the PBE functional using various basis sets. CP denotes use of the counter-poise correction method.

observations for the molecular stacks in crystalline NiPc.[44] Therefore, for NiPc the equilibrium geometry was deduced from the minimum of the binding energy curve. A full relaxation with the PBE+vdW functional has indeed confirmed that the monomers remain planar. As noted above, for the MgPc dimer the monomers do not remain planar.[45,46] Therefore, for this system a full geometry relaxation has additionally been carried out with all functionals used, so as to obtain realistic geometries.

The basis set convergence of our calculations was verified by direct comparison of the eigenvalues and binding energies obtained from PBE calculations of a MgPc dimer comprising two planar MgPc molecules at an interplanar distance of 4 Å, using both FHI-aims and Gaussian with the basis sets specified above. The two spectra were in good agreement with a maximal difference of 0.0065 eV and a mean error of 0.002 eV (the latter is equivalent to a relative mean error of 0.06%), for all eigenvalues larger than −15 eV. The binding energy obtained using the Gaussian code with the CP-corrected cc-pVTZ basis set was smaller by 20 meV than the value obtained using the FHI-aims code with the tier2 basis set, and smaller by 13 meV than that obtained with the tier3 basis set, which essentially recovers the complete basis set limit.

For additional insights into basis set convergence issues, Figure 2 shows binding energy curves of the MgPc dimer, calculated with PBE using a smaller, double-ζ (DZ) level basis set, consisting of an all electron cc-pVTZ basis set for the Mg atoms and the 6-31G(d,p) basis set for the H,C, and N atoms. Using a DZ basis set leads to an overbinding of 0.25 eV relative to the FHI-aims tier2 basis set and yields an intermolecular distance of 3.7 Å, as compared to 4.0 Å with the tier2 basis set. The CP procedure overcorrects this overbinding and results in an underbinding of 0.06 eV and an intermolecular distance of 4.3 Å. The larger, triple-ζ (TZ) basis set yields a distance of 4.0 Å, in agreement with the FHI-aims tier2 result. As expected, its CP correction is much smaller and reduces the binding energy by 0.05 eV, overcorrecting by only 0.02 eV compared to the tier2 basis. This close agreement between results obtained using different types of basis sets within different codes shows that our results are well-converged. Basis set convergence tests for the M06 functional are discussed in the Supporting Information (SI). Importantly, we note that reliance on DZ basis sets may lead to spurious agreement between M06 and PBE+vdW binding energy curves, whereas the CP-corrected TZ basis set calculations reveal pronounced differences between the two curves, which are elaborated below. We note that while our TZ and tier 2 NAO calculations are sufficiently converged, BSSE errors can also be reduced substantially using diffuse functions. We have not utilized this route here because for the large systems studied in this work we have found that this introduces severe convergence difficulties.

3. Results and Discussion

Because we aim at a treatment of both the equilibrium electronic structure and the long-range dispersive interactions, we start our analysis by choosing which functionals are the most promising candidates for providing such a comprehensive treatment. For examining the TS-vdW C_6/R^6 correction scheme, we focus primarily on PBE and the PBE-hybrid as a prototypical semilocal and hybrid functional, respectively. We are well aware that B3LYP is likely the most popular choice for a hybrid functional but even so prefer the PBE-hybrid for several reasons. First, the PBE-hybrid and B3LYP yield essentially indistinguishable spectra for metal−phthalocyanines (ref 32 and cf. Figures 5 and 7 below), so we prefer to introduce as little empiricism as possible. This is especially so given that the PBE-hybrid has other advantages over B3LYP, e.g., yielding the correct result for the uniform electron gas limit and doing significantly better at predicting solid state atomization energies.[31,63] Furthermore, as noted above the range of dispersion interaction covered by the PBE-hybrid is somewhat higher than that of B3LYP. Nevertheless, because of its prominence in applications we do provide B3LYP results as well.

Next, we assess, using the NiPc electronic structure, which of the M06 family of functionals we should pursue. This family, constructed by Zhao and Truhlar,[17] consists of four different functionals, denoted as M06 (fractional Fock exchange), M06L (fully semilocal treatment of exchange, i.e., no fractional Fock exchange), M06−2X (with twice as much Fock exchange as in M06), and M06-HF (with 100% Fock exchange). Of those, M06 was recommended by Zhao and Truhlar for systems involving both transition metal chemistry and noncovalent interactions,[17] but it is instructive to consider the accuracy of the electronic structure obtained with other functionals of the M06 family. We additionally examine the electronic structure obtained from the revPBE GGA, primarily because the above-discussed "vdW-DFT" functional is based on it.

Figure 3 shows calculated eigenvalue spectra of the NiPc monomer, as well as the same spectra broadened by convolution with a 0.35 eV Gaussian to simulate the effective experimental resolution of ultraviolet photoemission spectroscopy (UPS) experiments performed by Ellis et al. on NiPc thin films,[64] also shown in the figure. We note that, strictly speaking, Kohn−Sham eigenvalues are not equivalent to quasiparticle excitation energies even if the exact xc functional is used.[31] Nevertheless, if a suitable approximate xc functional is used, they are often good approximations to electron removal energies.[31,33c,65] The figure compares the

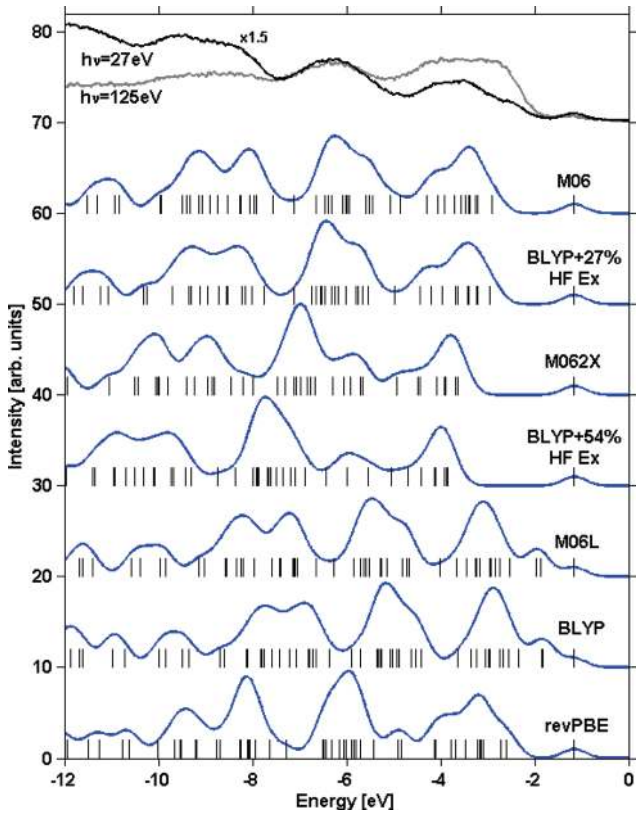

Figure 3. Computed NiPc single molecule spectra, calculated with revPBE, different M06-variants, and BLYP-based single-parameter hybrid exchange-correlation functionals. Raw eigenvalue data, as well as the same data broadened by a 0.35 eV Gaussian, are shown. This facilitates comparison with the UPS data of Ellis et al.,[64] obtained for a 11.8 Å NiPc film at $\theta = 70°$, also shown in the figure.

results of three M06 variants with corresponding one-parameter hybrids[66] based on BLYP,[58] a semiempirical GGA functional. To examine the role of exchange, in each case the M06-variant result is compared to a BLYP-based hybrid that has the same the fraction of Fock exchange. Two trends are immediately obvious: First, whereas the M06 spectrum agrees well with experiment, M06L and M06−2X yield spectra that do not. This agrees with the recommendation of Zhao and Truhlar. Second, the M06-variant spectra are remarkably similar (though, of course, not identical) to the corresponding BLYP-hybrid ones. This shows that, despite the many additional fitting parameters used in any M06 variant, the dominant factor in determining the electronic structure is the fraction of Fock exchange. In turn, the spectra obtained with BLYP and with BLYP+27% Fock exchange are remarkably similar to previously published spectra (ref 32 and cf. Figure 5 below), obtained with the nonempirical PBE and PBE-hybrid (i.e., 25% Fock exchange) functionals, respectively, further underscoring the dominant role of Fock exchange. Therefore, of the entire M06 family, only M06 is considered hereafter.

Interestingly, the leading (HOMO) and second peak of the revPBE spectrum are much closer to the spectra obtained from the hybrid functionals (BLYP+27% Fock exchange and M06) than to those obtained from the semilocal functionals (BLYP and M06L). We have observed a similar behavior

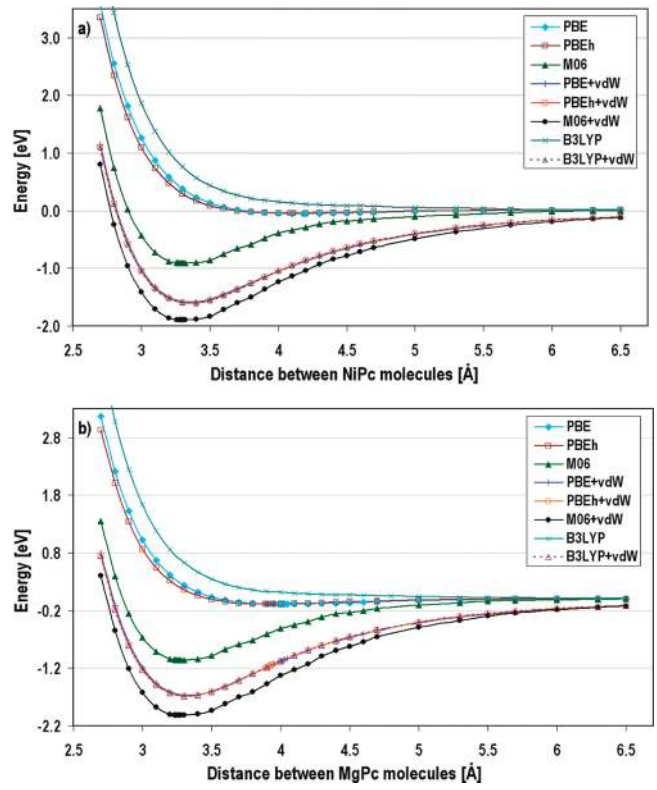

Figure 4. Binding energy curves, obtained with different exchange-correlation density functionals, for (a) NiPc and (b) MgPc dimers, composed of planar molecules.

for other MPc's (not shown for brevity). Likely, this is at least partly because the exchange enhancement factor of revPBE was constructed by fitting to exact exchange-only calculations of total atomic energies.[67] This compensates to some extent for self-interaction errors and thus improves the fit to experiment in the higher-lying part of the spectrum. However, this comes at the price of distorting the shape of the third and fourth peaks. Because revPBE, while better than other GGAs in this respect, still fails to yield a satisfactory electronic spectrum, we do not discuss it further here.

We now turn to the binding energy curves of NiPc and MgPc dimers, shown in Figure 4, obtained using the PBE, PBE-hybrid, B3LYP, and M06 functionals, with and without the C_6/R^6 correction. Clearly, the uncorrected PBE and PBE-hybrid calculations underestimate considerably the strength of the noncovalent interaction and overestimate the intermolecular distance in both dimers. The B3LYP calculations reveal no net attraction at all. This is a known tendency of semilocal and conventional hybrid functionals that has been demonstrated repeatedly for various systems (see, e.g., refs 1, 2, 13, 14, 19, 20, 22, 26). For both dimers, M06 significantly improves upon the semilocal and hybrid functionals, yielding binding energies that are higher by about 1.0 eV. However, the binding energies obtained with PBE+vdW, PBE-hybrid+vdW, and B3LYP+vdW are higher yet, by ∼0.7 eV as compared to M06. This difference between the TS-vdW corrected results and M06 is larger than the level of accuracy found in recent M06 studies of smaller dispersively bound systems,[55,68] likely due to the sheer size of the MPc molecules and the contribution of the π−d

Table 1. Intermolecular Distance in the NiPc and MgPc Dimers and Mg Atom Shift out of the Molecular Plane for the Latter[a]

	NiPc intermolecular distance [Å]	MgPc intermolecular distance [Å]	Mg atom shift [Å]
expt	3.24 [44]	3.172 (120 K), 3.185 (260 K) [45]	0.613 (120 K), 0.454 (260 K) [45]
PBE	4.2	3.79	0.88
PBE-hybrid	4.1	3.73	0.86
M06	3.30	3.30	0.61
PBE+vdW	3.22	3.29	0.56

[a] Calculated with the PBE, PBE-hybrid, M06, and vdW-corrected PBE functionals, compared to experimental values.

interaction. Furthermore, this difference can be traced back to the long-range behavior of the M06 functional, which is essentially the same as that of PBE or PBE-hybrid at intermolecular distances larger than 5.5 Å. For some applications, the latter difference may be practically unimportant if the near-equilibrium region is well-described. However, it is fundamentally important to realize that the hybrid meta-GGA approach does not possess the correct asymptotic behavior. This limitation may manifest itself practically as well, e.g., in systems where a cumulative effect of many long-range dispersive interactions is important.

For both dimers, the addition of the C_6/R^6 correction to the M06 functional recovers the correct long-range behavior and does not affect the equilibrium intermolecular distance. However the binding energy increases by ~1.0 eV, becoming ~0.3 eV larger than with PBE+vdW or PBE-hybrid+vdW. We note that the remaining difference may be attributed to the employed damping function. Since M06 already provides considerable attraction at the intermediate range, it may require a different model for the damping function. Without experimental or high-level quantum-chemical data for the binding energy, it is hard to say which functional yields a more accurate binding energy. However, the difference between PBE+vdW or PBE-hybrid+vdW and M06+vdW is significantly reduced (0.3 eV) as compared to the difference between uncorrected M06 and PBE(-hybrid)+vdW (0.7 eV).

To understand how well the approaches studied here do at geometry prediction, we have computed the equilibrium intermolecular distances obtained for the NiPc and MgPc dimers, as well as the shift of the Mg atom from the molecular plane for the latter. The computed values, compared to experimental data, are given in Table 1 (additional data on single molecule bond lengths and angles are given in the SI). As discussed above, PBE and PBE-hybrid significantly overestimate the equilibrium intermolecular distance of both dimers, whereas M06 and PBE+vdW yield values that are in good agreement with the experimental ones. The distance of the Mg atom from the molecular plane is underestimated by PBE and PBE-hybrid by ~0.3 Å, whereas it is within ~0.1 Å from experiment with PBE+vdW and within ~0.15 Å with M06. Full relaxation was not performed for M06+vdW, since the latter functional is not implemented in FHI-aims. However, on the basis of the binding energy curve of the planar dimer, we expect only minor changes from the uncorrected M06 dimer geometry.

Having accounted for dispersive interactions such that the correct equilibrium geometry was obtained, we now return to the electronic structure. Figure 5 shows calculated eigenvalue spectra of the NiPc dimer, as well as the same

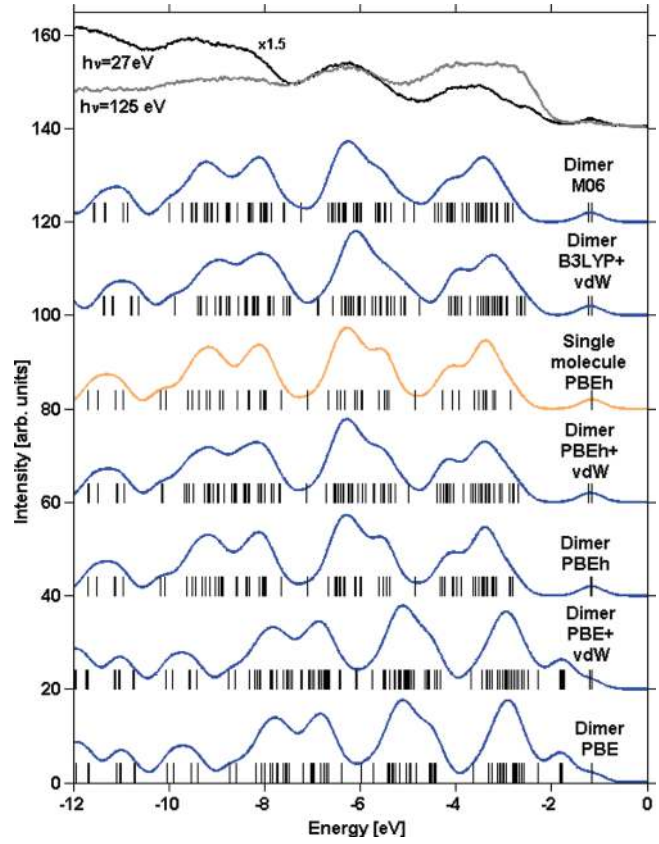

Figure 5. NiPc single molecule (orange online) and dimer (blue online) spectra, calculated with different exchange-correlation functionals and broadened by a 0.35 eV Gaussian, compared to the UPS data of Ellis et al.,[64] obtained for a 11.8 Å NiPc film at $\theta = 70°$. The dimer eigenvalues shown are those obtained for the equilibrium geometry specified in Table 1, except for the PBE-hybrid+vdW and B3LYP+vdW eigenvalues that were calculated for the geometry obtained with PBE+vdW.

spectra broadened by convolution with a 0.35 eV Gaussian to simulate the effective experimental resolution of ultraviolet photoemission spectroscopy (UPS). The calculated spectra are compared to the single molecule spectrum calculated with PBE-hybrid, as well as to the thin film UPS data of Ellis et al.,[64] also shown in the figure.

As expected, the dimer PBE-hybrid spectrum is similar to that of the single molecule, with some level splitting due to the interaction between the two molecules. In previous work, it was shown that for the NiPc single molecule, as well as for other transition metal Pc's, the PBE functional fails qualitatively, primarily because of underbinding of localized orbitals due to self-interaction errors.[32] A similar picture is revealed for the NiPc dimer, where the spectra calculated with the hybrid functionals, PBE-hybrid and M06,

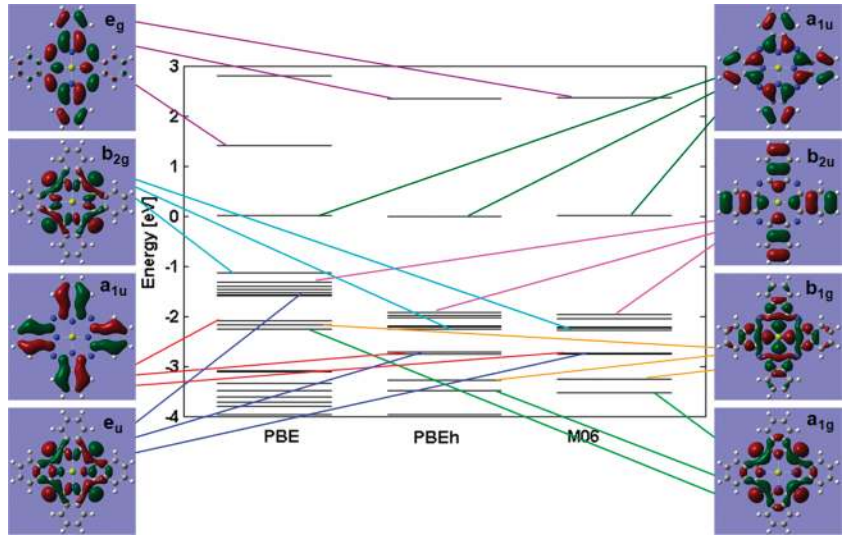

Figure 6. Energy and ordering of selected MgPc molecular orbitals, calculated with different exchange-correlation functionals. All spectra were shifted so as to align the highest occupied molecular orbital (HOMO). For clarity, only one example of each doubly degenerate e_g and e_u orbital is shown.

agree with experiment even at the overestimated intermolecular distance of 4.1 Å (obtained with the uncorrected PBE-hybrid). Contrary to the hybrid spectra, the PBE spectra are quite different from experiment. An obvious difference from experiment is that the PBE spectrum is "compressed"; i.e., there is a general narrowing of the gaps between peaks and more energy levels are "squeezed" into a given energy window. "Compression" of experimental spectra is a well-known tendency of semilocal functionals, which can be attributed to the comparison of Kohn−Sham eigenvalues with quasiparticle excitation energies.[31,69,70] (Note that in a hybrid calculation, unlike in a "true" Kohn−Sham one, one makes use of a nonlocal potential that can mimic the nonlocal self-energy. This may avoid the "compression" problem.[31,32]) Moreover, in the PBE spectrum there is a spurious peak between the experimentally observed first and second peaks and the subfeatures for the second peak are missing. This PBE distortion of the line shape remains with PBE+vdW geometry, but the PBE-hybrid+vdW and B3LYP+vdW retain the correct electronic structure.[47]

Figure 6 shows the eigenvalues of the MgPc molecule, obtained with different functionals, together with selected molecular orbitals and their energy positions. In agreement with trends observed for other transition metal Pc's,[32] the PBE spectrum of MgPc also appears to be affected by SIE. The b_{2g}, e_u, b_{1g}, and a_{1g} orbitals, localized over the central region of the molecule, are shifted to higher energies compared to the hybrid spectra, leading to a distortion of the PBE spectrum.

Figure 7 shows the calculated eigenvalue spectra of the MgPc dimer, as well as the same spectra, broadened by convolution with a 0.35 eV Gaussian to simulate the effective experimental resolution of UPS. Single molecule spectra obtained with PBE and PBE-hybrid are also shown. As expected, the dimer spectra are similar to those of the single molecule, obtained with the same functional, with some level splitting due to the interaction between the two molecules. Similarly to NiPc, the PBE spectra obtained for the PBE and PBE+vdW geometries appear compressed compared to

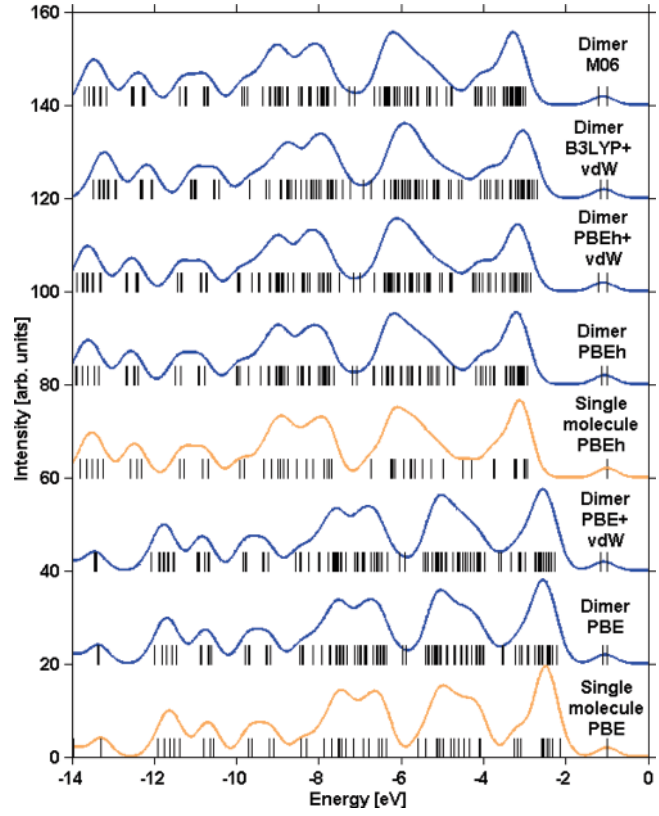

Figure 7. MgPc single molecule (orange online) and dimer (blue online) spectra, calculated with different exchange-correlation functionals and broadened by a 0.35 eV Gaussian. The dimer eigenvalues shown are those obtained for the equilibrium geometry specified in Table 1, except for the PBE-hybrid+vdW and B3LYP+vdW eigenvalues that were calculated for the geometry obtained with PBE+vdW.

the hybrid spectra. However, the differences in the line shape between the PBE and the hybrid calculations are not as visually obvious for MgPc as they are for NiPc, at least at the broadening level used.[71] Still, on the basis of the qualitative differences in molecular orbital ordering shown

in Figure 6, as well as on previous work on identifying self-interaction errors in similar[32] and other[33] organic molecules, we believe that the hybrid calculations are more reliable. A comparison against high-resolution experimental data could provide a definitive answer, should such data become available.

Even though PBE+vdW yields accurate geometries for the noncovalently bound systems studied here, it still fails to give a good description of the electronic structure, primarily due to self-interaction errors, whereas hybrid functionals yield spectra that are in good agreement with experiment (for NiPc) even with overestimated intermolecular distances. For both the NiPc and MgPc dimers, M06 provides good accuracy for the geometry and the electronic structure, but M06 does not capture the long-range asymptotics and yields a binding energy significantly lower than those obtained with the TS-vdW correction.

We therefore propose the following scheme for DFT calculations of systems involving noncovalent interactions: First, geometry relaxation can be performed with a PBE+vdW calculation, which is computationally less demanding than a corresponding PBE-hybrid+vdW calculation, yet yields binding energy curves that are practically identical to those obtained with the latter and in good agreement with pertinent experiments. This step is then to be followed by a calculation with the PBE-hybrid functional in order to obtain reliable electronic structure data.[72] Such a scheme is expected to provide a treatment of noncovalent interactions on the one hand and the electronic structure on the other hand. Since it is not based on a particular training set, it can be applied robustly to a wide range of materials.

4. Conclusion

The binding energy curves, geometry, and electronic structure of NiPc and MgPc dimers were calculated using the PBE, PBE-hybrid, B3LYP, and M06 functionals with and without a first principles C_6/R^6 correction. The PBE and PBE-hybrid functionals, inherently unsuitable for treating dispersive interactions, significantly underestimate the strength of the $\pi-$d and $\pi-\pi$ interactions in the NiPc and MgPc dimers, respectively. Unlike PBE and PBE-hybrid, both M06 and PBE+vdW yield geometries in good agreement with experiment. However, PBE+vdW seriously distorts the electronic structure due to self-interaction errors.[47] Conversely, M06 does very well for the electronic structure but its binding energy is significantly different from that of PBE+vdW. This difference, which is accentuated by the sheer size of the system, reflects the fact that M06 does not possess the correct R^{-6} asymptote. Correcting the long-range dispersion brings M06 into much better agreement with PBE+vdW.

The binding energy curves obtained with PBE-hybrid+vdW are essentially indistinguishable from those obtained with PBE+vdW; i.e., both functionals possess the correct asymptotic behavior and do equally well on the geometry. But unlike PBE, PBE-hybrid (as well as B3LYP) mitigates the self-interaction errors and also describes the electronic structure well. Still, relaxation with PBE+vdW is less computationally intensive due to the absence of Fock exchange. Thus, although one can perform the entire calculation with the PBE-hybrid+vdW or the B3LYP+vdW scheme, it is often preferable in practice to perform the relaxation with PBE+vdW, followed by computation of the electronic structure with the PBE-hybrid.

We conclude that the thorny problem of obtaining a description of both geometry and electronic structure can be generally overcome by decoupling the two issues. We choose a functional that is appropriate to the electronic structure, but does not include a good description of dispersive interactions (e.g., PBE-hybrid), and augment it with first principles corrections for the leading terms of the dispersion interaction using the TS-vdW approach. This provides a robust and efficient scheme which we believe will find much use in future studies of organic electronic materials.

Acknowledgment. Work at the Weizmann Institute was supported by the Israel Science Foundation, the Gerhard Schmidt Minerva Center for Supra-Molecular Architecture, the Lise Meitner Center for Computational Chemistry, and the historical generosity of the Perlman family. We thank T. S. Ellis and K. T. Park (Baylor University) for kindly providing their photoemission data and J. M. L. Martin (Weizmann Institute) for helpful discussions and for kindly providing us with M06 binding energies for the S22 data set. A.T. acknowledges financial support from the Alexander von Humboldt (AvH) foundation.

Supporting Information Available: Two figures and a table show additional information. This material is available free of charge via the Internet at http://pubs.acs.org.

References

(1) Kristyán, S.; Pulay, P. *Chem. Phys. Lett.* **1994**, *229*, 175.

(2) Pérez-Jordá, J. M.; Becke, A. D. *Chem. Phys. Lett.* **1995**, *233*, 134.

(3) (a) Langreth, D. C.; Perdew, J. P. *Solid State Commun.* **1975**, *17*, 1425. (b) Langreth, D. C.; Perdew, J. P. *Phys. Rev. B* **1977**, *15*, 2884.

(4) Aryasetiawan, F.; Miyake, T.; Terakura, K. *Phys. Rev. Lett.* **2002**, *88*, 166401.

(5) Fuchs, M.; Gonze, X. *Phys. Rev. B* **2002**, *65*, 235109.

(6) (a) Furche, F.; van Voorhis, T. *J. Chem. Phys.* **2005**, *122*, 164106. (b) Furche, F. *J. Chem. Phys.* **2008**, *129*, 114105.

(7) Marini, A.; García-González, P.; Rubio, A. *Phys. Rev. Lett.* **2006**, *96*, 136404.

(8) Harl, J.; Kresse, G. *Phys. Rev. B* **2008**, *77*, 045136.

(9) Rohlfing, M.; Bredow, T. *Phys. Rev. Lett.* **2008**, *101*, 266106.

(10) Janesko, B. G.; Henderson, T. M.; Scuseria, G. E. *J. Chem. Phys.* **2009**, *130*, 081105.

(11) Toulouse, J.; Gerber, I. C.; Jansen, G.; Savin, A.; Ángyán, J. G. *Phys. Rev. Lett.* **2009**, *102*, 096404.

(12) Kohn, W.; Meir, Y.; Makarov, D. E. *Phys. Rev. Lett.* **1998**, *80*, 4153.

(13) Dion, M.; Rydberg, H.; Schröder, E.; Langreth, D. C.; Lundqvist, B. I. *Phys. Rev. Lett.* **2004**, *92*, 246401.

(14) Adamo, C.; Barone, V. *J. Chem. Phys.* **1998**, *108*, 664.

(15) Kurita, N.; Inoue, H.; Sekino, H. *Chem. Phys. Lett.* **2003**, *370*, 161.

(16) Xu, X.; Goddard, W. A. *Proc. Natl. Acad. Sci.* **2004**, *101*, 2673.

(17) Zhao, Y.; Truhlar, D. G. *Acc. Chem. Res.* **2008**, *41*, 157. Zhao, Y.; Truhlar, D. G. *Theor. Chem. Acc.* **2008**, *120*, 215.

(18) (a) Tarnopolsky, A.; Karton, A.; Sertchook, R.; Gruzman, D.; Martin, J. M. L. *J. Phys. Chem. A* **2008**, *112*, 3. (b) Karton, A.; Tarnopolsky, A.; Lamère, J. F.; Schatz, G. C.; Martin, J. M. L. *J. Phys. Chem. A* **2008**, *112*, 12868.

(19) Wu, X.; Vargas, M. C.; Nayak, S.; Lotrich, V.; Scoles, G. *J. Chem. Phys.* **2001**, *115*, 8748.

(20) Wu, Q.; Yang, W. *J. Chem. Phys.* **2002**, *116*, 515.

(21) Johnson, E. R.; Becke, A. D. *J. Chem. Phys.* **2005**, *123*, 024101.

(22) (a) Neumann, M. A.; Perrin, M.-A. *J. Phys. Chem.* **2005**, *109*, 15531. (b) Neumann, M. A.; Leusen, F. J. J.; Kendrick, J. *Angew. Chem., Int. Ed.* **2008**, *47*, 2427.

(23) Nara, J.; Higai, S.; Morikawa, Y.; Ohno, T. *J. Chem. Phys.* **2004**, *120*, 6705.

(24) Grimme, S. *J. Comput. Chem.* **2006**, *27*, 1787.

(25) Jurečka, P.; Èerny, J.; Hobza, P.; Salahub, D. R. *J. Comput. Chem.* **2007**, *28*, 555.

(26) Tkatchenko, A.; von Lilienfeld, O. A. *Phys. Rev. B* **2008**, *78*, 045116.

(27) Silvestrelli, P. L. *Phys. Rev. Lett.* **2008**, *100*, 053002.

(28) Tkatchenko, A.; Scheffler, M. *Phys. Rev. Lett.* **2009**, *102*, 073005.

(29) Byrd, E. F. C.; Scuseria, G. E.; Chabalowski, C. F. *J. Phys. Chem. B* **2004**, *108*, 13100.

(30) Perdew, J. P.; Zunger, A. *Phys. Rev. B* **1981**, *23*, 5048.

(31) Kümmel, S.; Kronik, L. *Rev. Mod. Phys.* **2008**, *80*, 3.

(32) (a) Marom, N.; Hod, O.; Scuseria, G. E.; Kronik, L. *J. Chem. Phys.* **2008**, *128*, 164107. (b) Marom, N.; Kronik, L. *Appl. Phys. A: Mater. Sci. Process.* **2009**, *95*, 159.

(33) (a) Dori, N.; Menon, M.; Kilian, L.; Sokolowski, M.; Kronik, L.; Umbach, E. *Phys. Rev. B* **2006**, *73*, 195208. (b) Arantes, J. T.; Lima, M. P.; Fazzio, A.; Xiang, H.; Wei, S.-H.; Dalpian, G. M. *J. Phys. Chem. B* **2009**, *113*, 5376. (c) Körzdörfer, T.; Kümmel, S.; Marom, N.; Kronik, L. *Phys. Rev. B* **2009**, *79*, R201205. (d) Palummo, M.; Hogan, C.; Sottile, F.; Bagalá, P.; Rubio, A. *J. Chem. Phys.* **2009**, *131*, 084102.

(34) Naturally, one may go beyond DFT and use schemes like MP2+ΔvdW for obtaining the relaxed geometry. See Tkatchenko, A.; DiStasio, R. A., Jr; Head-Gordon, M.; Scheffler, M. *J. Chem. Phys.* **2009**, *131*, 094106. and many-body methods (quasiparticle excitations) for calculating the electronic structure.

(35) See, e.g., (a) Puzder, A.; Dion, M.; Langreth, D. C. *J. Chem. Phys.* **2006**, *124*, 164105. (b) Kleis, J.; Lundqvist, B. I.; Langreth, D. C.; Schröder, E. *Phys. Rev. B* **2007**, *76*, 100201. (c) Cooper, V. R.; Thonhauser, T.; Puzder, A.; Schröder, E.; Lundqvist, B. I.; Langreth, D. C. *J. Am. Chem. Soc.* **2008**, *130*, 1304. (d) Cooper, V. R.; Thonhauser, T.; Langreth, D. C. *J. Chem. Phys.* **2008**, *128*, 204102. (e) Hooper, J.; Cooper, V. R.; Thonhauser, T.; Romero, N. A.; Zerilli, F.; Langreth, D. C. *ChemPhysChem* **2008**, *9*, 891. (f) Lazić, P.; Crljen, Ž.; Brako, R.; Gumhalter, B. *Phys. Rev. B* **2005**, *72*, 245407. (g) Yanagisawa, S.; Lee, K.; Morikawa, Y. *J. Chem. Phys.* **2008**, *128*, 244704. (h) Sony, P.; Puschnig, P.; Nabok, D.; Ambrosch-Draxl, C. *Phys. Rev. Lett.* **2007**, *99*, 176401.

(36) Zhang, Y.; Yang, W. *Phys. Rev. Lett.* **1998**, *80*, 890.

(37) (a) Vydrov, O. A.; Wu, Q.; Voorhis, T. V. *J. Chem. Phys.* **2008**, *129*, 014106. (b) Gulans, A.; Puska, M. J.; Nieminen, R. M. *Phys. Rev. B* **2009**, *79*, 201105.

(38) (a) Dobson, J. F.; McLennan, K.; Rubio, A.; Wang, J.; Gould, T.; Le, H. M.; Dinte, B. P. *Aust. J. Chem.* **2001**, *54*, 513. (b) Dobson, J. F.; White, A.; Rubio, A. *Phys. Rev. Lett.* **2006**, *96*, 073201.

(39) (a) Perdew, J. P.; Burke, K.; Ernzerhof, M. *Phys. Rev. Lett.* **1996**, *77*, 3865. (b) Perdew, J. P.; Burke, K.; Ernzerhof, M. *Phys. Rev. Lett.* **1997**, *78*, 1396 (E).

(40) (a) Perdew, J. P.; Ernzerhof, M.; Burke, K. *J. Chem. Phys.* **1996**, *105*, 9982. (b) Adamo, C.; Barone, V. *J. Chem. Phys.* **1999**, *110*, 6158. (c) Ernzerhof, M.; Scuseria, G. E. *J. Chem. Phys.* **1999**, *110*, 5029.

(41) (a) Stephens, P. J.; Devlin, F. J.; Chabalowski, C. F.; Frisch, M. J. *J. Phys. Chem.* **1994**, *98*, 11623. (b) Becke, A. D. *J. Chem. Phys.* **1993**, *98*, 5648.

(42) Applications of Phthalocyanines. In *The Porphyrin Handbook*, 1st ed.; Kadish, K. M., Smith, R., Guilard R., Eds.; Academic Press: San Diego, CA, 2003; *Vol 19*.

(43) Grimme, S. *Angew. Chem., Int. Ed.* **2008**, *47*, 3430.

(44) Schramm, C. J.; Scaringe, R. P.; Stojakovic, D. R.; Hoffman, B. M.; Ibers, J. A.; Marks, T. J. *J. Am. Chem. Soc.* **1980**, *102*, 6702.

(45) Janczak, J.; Kubiak, R. *Polyhedron* **2001**, *20*, 2901.

(46) (a) Mizuguchi, J. *J. Phys. Chem. A* **2001**, *105*, 1121. (b) Mizuguchi, J. *J. Phys. Chem. A* **2001**, *105*, 10719.

(47) At a given geometry, the "+vdW" part of the computation has no effect on the electronic structure by construction, as it is only added to the total energy. However, because the optimized geometry with the vdW corrections differs from the uncorrected one, some geometry-dependent changes in the electronic structure may ensue.

(48) Santra, B.; Michaelides, A.; Fuchs, M.; Tkatchenko, A.; Filippi, C.; Scheffler, M. *J. Chem. Phys.* **2008**, *129*, 194111.

(49) Chu, X.; Dalgarno, A. *J. Chem. Phys.* **2004**, *121*, 4083.

(50) Hirshfeld, F. L. *Theor. Chim. Acta* **1977**, *44*, 129.

(51) Nalewajski, R. F.; Parr, R. G. *Proc. Natl. Acad. Sci. U.S.A.* **2000**, *97*, 8879.

(52) (a) Johnson, E. R.; Becke, A. D. *Chem. Phys. Lett.* **2006**, *432*, 600. (b) Becke, A. D.; Johnson, E. R. *J. Chem. Phys.* **2007**, *127*, 124108.

(53) Jurečka, P.; Šponer, J.; Černy, J.; Hobza, P. *Phys. Chem. Chem. Phys.* **2006**, *8*, 1985.

(54) The s_R values found for PBE and PBE-hybrid are smaller than those found in conjunction with empirical determination of C_6 coefficients because we use *free-atom* vdW radii, which yield larger effective radii than the values reported by Bondi: Bondi, A. J. *J. Phys. Chem.* **1964**, *68*, 441.

(55) Karton, A.; Gruzman, D.; Martin, J. M. L. *J. Phys. Chem. A* **2009**, *113*, 8434.

(56) (a) Blum, V.; Gehrke, R.; Hanke, F.; Havu, P.; Havu, V.; Ren, X.; Reuter, K.; Scheffler, M. *Comput. Phys. Commun.* **2009**, *180*, 2175. (b) FHI-aims, Theory Department, Fritz-Haber Institute Berlin, http://www.fhi-berlin.mpg.de/aims/, accessed Jul 1, 2009.

(57) The calculations were performed using either revision C.01wis2 (2004) or revision E.01+MNG (2007) of the *Gaussian03* suite of programs . Frisch, M. J.; Trucks, G. W.; Schlegel, H. B.; Scuseria, G. E.; Robb, M. A.; Cheeseman, J. R.; Montgomery, J. A., Jr.; Vreven, T.; Kudin, K. N.; Burant, J. C.; Millam, J. M.; Iyengar, S. S.; Tomasi, J.; Barone, V.; Mennucci, B.; Cossi, M.; Scalmani, G.; Rega, N.; Petersson, G. A.; Nakatsuji, H.; Hada, M.; Ehara, M.; Toyota, K.; Fukuda, R.; Hasegawa, J.; Ishida, M.; Nakajima, T.; Honda, Y.; Kitao, O.; Nakai, H.; Klene, M.; Li, X.; Knox, J. E.; Hratchian, H. P.; Cross, J. B.; Bakken, V.; Adamo, C.; Jaramillo, J.; Gomperts, R.; Stratmann, R. E.; Yazyev, O.; Austin, A. J.; Cammi, R.; Pomelli, C.; Ochterski, J. W.; Ayala, P. Y.; Morokuma, K.; Voth, G. A.; Salvador, P.; Dannenberg, J. J.; Zakrzewski, V. G.; Dapprich, S.; Daniels, A. D.; Strain, M. C.; Farkas, O.; Malick, D. K.; Rabuck, A. D.; Raghavachari, K.; Foresman, J. B.; Ortiz, J. V.; Cui, Q.; Baboul, A. G.; Clifford, S.; Cioslowski, J.; Stefanov, B. B.; Liu, G.; Liashenko, A.; Piskorz, P.; Komaromi, I.; Martin, R. L.; Fox, D. J.; Keith, T.; Al-Laham, M. A.; Peng, C. Y.; Nanayakkara, A.; Challacombe, M.; Gill, P. M. W.; Johnson, B.; Chen, W.; Wong, M. W.; Gonzalez, C.; Pople, J. A. *Gaussian03*; Gaussian, Inc.: Wallingford, CT, 2003.

(58) (a) Becke, A. D. *Phys. Rev. A* **1988**, *38*, 3098. (b) Lee, C.; Yang, W.; Parr, R. G. *Phys. Rev. B* **1988**, *37*, 785.

(59) Weigend, F.; Ahlrichs, R. *Phys. Chem. Chem. Phys.* **2005**, *7*, 3297.

(60) (a) Dunning, T. H., Jr. *J. Chem. Phys.* **1989**, *90*, 1007. (b) Woon, D. E.; Dunning, T. H., Jr. *EMSL Basis Set Exchange*; https://bse.pnl.gov/bse/portal, accessed Apr 27, 2008.

(61) Boys, S. F.; Bernardi, F. *Mol. Phys.* **1970**, *19*, 553.

(62) Simon, S.; Duran, M.; Dannenberg, J. J. *J. Chem. Phys.* **1996**, *105*, 11024.

(63) Paier, J.; Marsman, M.; Kresse, G. *J. Chem. Phys.* **2007**, *127*, 024103.

(64) Ellis, T. S.; Park, K. T.; Ulrich, M. D.; Hulbert, S. L.; Rowe, J. E. *J. Appl. Phys.* **2006**, *100*, 093515.

(65) Chong, D. P.; Gritsenko, O. V.; Baerends, E. J. *J. Chem. Phys.* **2002**, *116*, 1760. (b) Gritsenko, O. V.; Baerends, E. J. *J. Chem. Phys.* **2002**, *117*, 9154.

(66) See eq 75 in ref 31.

(67) For dispersively bound systems, the similarity of revPBE exchange to exact exchange was discussed, e.g., in the context of the binding energy curve of the Kr dimer. See Langreth, D. C.; Dion, M.; Rydberg, H.; Schröder, E.; Hyldgaard, P.; Lundqvist, B. I. *Int. J. Quantum Chem.* **2005**, *101*, 599.

(68) (a) Hohenstein, E. G.; Chill, S. T.; Sherrill, C. D. *J. Chem. Theor. Comput.* **2008**, *4*, 1996. (b) Raju, R. K.; Ramraj, A.; Hillier, I. H.; Vincent, M. A.; Burton, N. A. *Phys. Chem. Chem. Phys.* **2009**, *11*, 3411.

(69) Hybertsen, M. S.; Louie, S. G. *Phys. Rev. B* **1986**, *34*, 5390.

(70) Jones, R. O.; Gunnarsson, O. *Rev. Mod. Phys.* **1989**, *61*, 689.

(71) A similar trend was observed previously for FePc and MnPc. See Marom, N.; Kronik, L. *Appl. Phys. A: Mater. Sci. Process.* **2009**, *95*, 165.

(72) Calculations of quasiparticle excitations at the optimized geometry may also be performed.

CT900410J